earth

MDPI

Article

Biomass burning and water balance dynamics in the Lake Chad Basin of Africa

Forrest W Black[1], Jejung Lee[2*], Charles M Ichoku[3], Luke Ellison[4], Charles K Gatebe[5], RakiyaBabamaaji[6], KhodayarAbdollahi[7], Soma San[8],

[1] Department of Earth and Environmental Sciences,University of Missouri – Kansas City; fwbr3d@mail.umkc.edu

[2] Department of Earth and Environmental Sciences,University of Missouri – Kansas City; leej@umkc.edu

[3] Graduate Program, College of Arts & Sciences, Howard University; charles.ichoku@howard.edu

[4] Science Systems and Applications, Inc.; lukecaj@gmail.com

[5] Universities Space Research Association Greenbelt; charles.k.gatebe@nasa.gov

[6] National Space Research and Development Agency (NASRDA; rakiya.babamaaji@gmail.com

[7] Shahrekord University; kabdolla@sku.ac.ir

[8] Department of Earth and Environmental Sciences, University of Missouri – Kansas City; ssaxk8@umkc.edu

* Correspondence: leej@umkc.edu; Tel.: 816-235-6495

Abstract: The present study investigates the effect of biomass burning on the water cycle using a case study of the Chari-Logone Catchment of Lake Chad Basin. The Chari-Logone catchment was selected since it supplies over 90% of the water input to the Lake, which is the largest basin in the NSSA. Two water balance simulations, one considering burning and one without, were compared from the years 2003 to 2011. For a more comprehensive assessment of the effects of burning, albedo change, which has been shown to have a significant impact on a number of environmental factors, was used as a model input for calculating potential evapotranspiration. Analysis of the burning scenario show that burning grassland, which composes almost 75% of Chari-Logone total land cover, causes increased ET and runoff during winter months. Recent studies have demonstrated the increasing trend in LCB of converting shrubland, grassland, and wetlands to cropland. This change from grassland to cropland has the potential of decreasing water available to water bodies during the winter. All vegetative classes in a burning scenario showed a decrease in ET during the wet season, supporting the idea that, with increased burning, there would be a severe decrease of precipitation.

Keywords: Lake Chad Basin; biomass burning; water balance; evapotranspiration; MODIS; albedo

Citation: Lastname, F.; Lastname, F.; Lastname, F. Title. *Earth* **2021**, *2*, Firstpage–Lastpage. https://doi.org/10.3390/xxxxx

Received: date
Accepted: date
Published: date

1. Introduction

The Lake Chad Basin (LCB) experienced a dramatic change in precipitation since the 1960s, which has drastically affected the size of Lake Chad [1]. Lake Chad gained widespread attention from the scientific communities and the general public due to its rapid shrinkage from 25,000 km^2 in 1963 to less than 3,000 km^2 in 2008 [2]. Lake Chad's shrinkage is significantly detrimental to regional sustainability as it is an economically important water resource that agricultural and fishing activities depend upon. In a series of surveys interviewing 25,000 households in the southwestern portion of the lake, 59%

of the households earned three-quarters of their income from farming, 36% earned income from a combination of fishing and farming, and 5% relied entirely on fishing [3]. A number of factors have been attributed to the Lake shrinkage, including decrease in precipitation [4], poor water management practices [5], and land use change [6].

Most of the rainfall in the LCB is immediately lost to ET [7] leaving the region sensitive to precipitation anomalies. Precipitation in the region is bi-seasonal with wet season monsoonal rains lasting from April to October and the dry season the rest of the year. The monsoonal rains are driven by the Intertropical Convergence Zone (ITCZ), created by the convergence of trade winds from the northern and southern hemispheres forming the ascending branch of the Hadley circulation [8]. Precipitation in the Sahel has been shown to be affected by the El Niño Southern Oscillation (ENSO) system, which is a cycle of ocean and atmospheric interaction that produces an irregularly periodic variation in winds and sea surface temperatures over the tropical eastern Pacific Ocean. During El Niño years, the wind pattern associated with the West African Monsoon has been shown to create a dry condition across the Sahel region leading to precipitation deficits [9]. High variability of rainfall due to these meteorological factors and other regional phenomena have contributed to a series of droughts in the 1970s and 1980s, with a gradual trend of annual rainfall recovery occurring since the 1990s contributing to Lake Chad recovery (Figure 1).

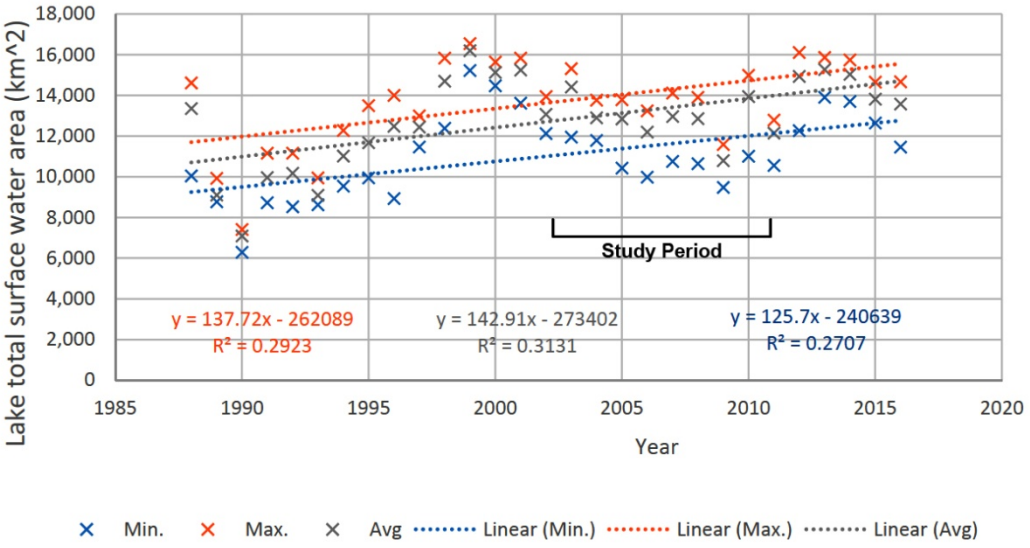

Figure 1. LCB regional cumulative rainfall anomalies taken from GPCP Stations from 1978 to 2014 [10]. Precipitation was more level during the 2003 – 2011 study period as indicated on the figure.

Another factor that has not been paid much of attention to is the occurrence of biomass burning, whether through wildfires or human induced burning. Biomass burning has been shown to have significant impacts on climate by altering land cover and vegetation [11–13], introducing aerosols and trace gases [14–15], and changing land surface characteristics, especially in regard to surface albedo [16–17]. Ichoku's study [18]of biomass burning in the NSSA, showed an increased conversion of shrubland, grassland, and wetlands to cropland from 2003 to 2013. This in turn affect the amount of biomass burning that occurs since prescribed burning is one of the primary sources of biomass burning in the NSSA. The study also found areas with relatively high burn activity experienced much higher evapotranspiration and posited a relationship between biomass burning

and increased precipitation. However, there have been no studies specifically in the LCB examining the relationship of burning and the water cycle.

The Chari-Logone catchment (CLC), a sub-basin of LCB, was chosen for this study as it provides 95% of the water input to Lake Chad and is the main driver for the entire lake system [19]. The Chari and Logone rivers provide an average of 1,946 mm/year to the lake whereas direct rainfall contributes a mere 329 mm annually [20]. The spatial extent of the study area is 601,350 km^2 and is located within the borders of Cameroon, Chad, Central African Republic, and Sudan. The catchment lies between 5° N and 15° N at the eastern part of the Sahel (Figure 2).

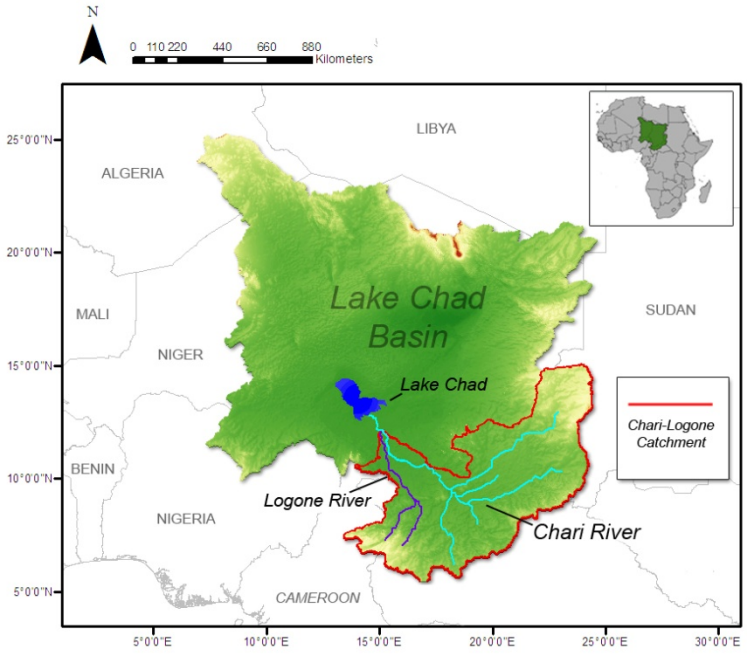

Figure 2. Map of Lake Chad Basin located in Sahelian Africa. The Catchment study region is outlined in red and located in the southeastern portion of the Basin.

A large contributor to biomass burning within the LCB is the use of fire to remove vegetative growth at the end of a growing season and the clearing of grassland and savanna for agricultural use. At the early to late dry season (November-March), a patch mosaic burning regime to clear unwanted vegetation has been used to clear savannah and woody areas of wild animals and facilitate clearing land for planting crops. Burning primarily occurs during the dry season when rainfall is at a minimum to clear the wet season's growth or to convert the land for future agricultural use. Aerosol byproducts of biomass burning have been known to produce significant amounts of black carbon, carbon monoxide, and carbon dioxide [14]. Furthermore, the resultant ash and charcoal deposition and change in land cover have been known to have a significant impact on surface albedo [16,21–22]. Surface albedo darkening from burning is caused by char deposition that increases absorption of solar radiation [23]. Desales [17] found that change in albedo coupled with a decrease in leaf area index (LAI) and vegetative land cover fraction from burning was linked to convective instability. The cause of this convective instability and precipitation loss is a cooling and drying of the atmosphere, leading to the weakening of upward atmospheric motion during the onset and mature stages of the monsoon.

Biomass burning effect on water cycle in the Sahel have been addressed to some degree in regard to ET, soil moisture, and precipitation, but conclusive evidence is limited by issues associated with burning and vegetative seasonality [18]. Other studies

associating water cycle changes with burning include its effect on soil infiltration rates, surface runoff [24], and soil erosion [25–26]. Previous studies on the water cycle of Sahelian regions use models focused on terrestrial water storage (TWS) using data from satellites such as Gravity Recovery and Climate Experiment (GRACE) [27–38]. While such models have helped to bring about great advances in understanding hydrologic dynamics on a climate scale, their spatial resolution is too coarse for detailed characterization of burned areas.

Lack of in situ data is largely due to the sparseness of meteorological stations and the fact that existing stations are inconsistent at recording data on a daily or even monthly basis [31–33]. Additionally, installing new stations is difficult in the LCB due to insecurity in the region. Water balance is the conservation of hydrologic inputs and outputs within a system. WetSpass, which stands for Water and Energy Transfer between Soil, Plants and Atmosphere under quasi-Steady State, is a physically based water balance model that is not as data intensive as other water balance models [34–35]. Babamaaji[6] demonstrated the effective use of WetSpass in the LCB.

A drawback of WetSpass is its inability to calculate water balance more frequent then seasonally. This however, has been addressed in the newer version, WetSpass-M [35], which was designed specifically to calculate monthly water balance.

WetSpass-M utilizes raster data and calculations are performed on a cell by cell basis where the input data is geospatially overlayed and sub-divided into vegetated, bare soil, open water, and impervious surface fraction. Water balance calculation of each pixel is processed in the following order: interception (process 1), surface runoff (process 2), evapotranspiration (process 3), and recharge (process 4) (Figure 3). Additionally, land-use/land-cover fraction values for each pixel are used as weighting factors for the calculation of the water balance [35].

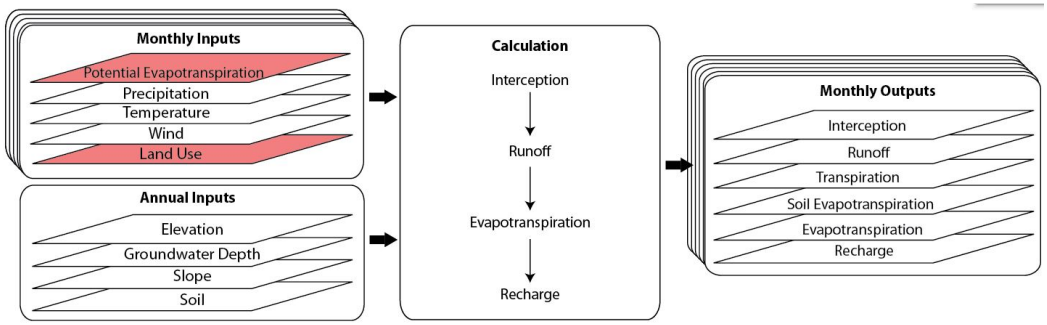

Figure 3. Schematic representation of WetSpass-M inputs and outputs. Data sets shown in red were adjusted to account for burning scenarios.

There has been little research on using a water balance model to calculate the effect of biomass burning on a hydrological system, especially in a data scarce region in Africa. In order to accomplish this, the present study investigates burning effects on the water balance in the LCB by incorporating burning parameters such as surface albedo and land cover characteristics of burned areas into a water balance model. The present water balance modeling approach determines how biomass burning affects regional scale water cycles and interpret if burning would affect the shrinkage of the lake. The time period chosen for this study is from 2003 to 2011 in order to use albedo change from burning as described by [16]. The study hopes to find a correlation between increased evapotranspiration or increased precipitation due to burning. If there is a correlation, what vegetative land types are most greatly affected? Supposing a continued conversion of other land use types to cropland, what does this imply for water balance in LCB? To answer these questions, it is necessary to use model to comparing how burning affects water balance within the LCB, particularly examining water balance change in vegetative areas. De-

termining which parameters are affected by burning and the percentage of land use within the study area are also important steps to building a comprehensive model.

2. Materials and Methods

2.1 The WetSpass-M: the water balance model

WetSpass-M has shown favorable results for modeling water balance in the western Sahel in the Black Volta Basin [35] and in Northern Africa [36]. Calculations for the resolution of the input land cover and soil raster imagery is important to influence sub-cell land cover heterogeneity as their classification is compared to a series of look-up tables for parameterization during water balance calculation [34]. The look up tables include land use and land cover, soil type, and rainy days per month. For this study, additional land cover parameters were included in the land use look up table to account for burning. These land cover parameters include LAI, vegetated area, burned area, impervious area, open water area, root depth, minimum stomata opening, vegetative height, Manning coefficient, land factor, and aerodynamic resistance. LAI change was calculated using the same method employed by[37]with original unburned vegetation cover, the fractional burned area, and vegetative survival rate as input parameters. Raster datasets required for input into WetSpass-M include precipitation, temperature, wind, soil, land cover, elevation, slope, and potential evapotranspiration (PET).The water balance model outputs are interception, actual evapotranspiration, surface runoff, recharge the summation of which are equal to precipitation. WetSpass-M calculates impervious or actual evapotranspiration (ET) using vegetation coefficients in conjunction with PET.

2.2 Datasets and parameters for burning

Ground station observations from the National Oceanic and Atmospheric Administration's (NOAA) National Center for Environmental Information (NCEI) database are available for sub-Saharan Africa. However, the stations in the study area are relatively few as compared to the United States or Europe and monthly or even yearly data is not always recorded for many stations. African stations are also not always accurate either due to instrument error or poor data management.

With such few ground stations, even if data is accurate, when the data is interpolated large areas within the study area, they are skewed based on spatial distribution. We, therefore, adopted the precipitation data from the NASA's Tropical Rainfall Measurement Mission (TRMM) https://disc.gsfc.nasa.gov/datasets/TRMM_3B31_7/summary. TRMM level 3 3B31was used for the study, with a 0.5 degree x 0.5 degree resolution at a monthly time scale and units in mm/month. The data covers the area from 40°N to 40°S latitude, and were collected from January 1998 to April 2015, shortly before the satellite re-entered Earth's atmosphere. A number of studies have examined the accuracy of TRMM data compared to station data in different regions [38–39]. One such study by Ojo and Omotosho[40] looked specifically at the accuracy of TRMM in Nigeria. The study found that TRMM performed very well when compared to the few meteorological stations available. TRMM did however have a tendency to marginally over estimate precipitation especially toward southwestern Nigeria, which is far from the study area.

Soil rasters were extracted from the United Nation's Food and Agriculture Organization (FAO) Harmonized World Soil Database (HWSD). HWSD was released in 2008 and is a 30 arc-second raster database with over 16,000 different soil mapping units that combine existing regional and national updates of soil information worldwide. Land

cover data were derived from MODIS MCD12Q1 Collection 6. This Level 3 dataset is a land classification raster created from an algorithm combining data from the Moderate Resolution Imaging Spectrometer (MODIS) instrument onboard NASA's Terra and Aqua satellites. The satellites were launched December 1999 and May 2002, respectively. An advantage of MODIS is its ability to capture images every 1-2 days with a 2,330 km wide swath. Thirty-six discrete spectral bands ranging in wavelengths from 0.4 μm to 14.4 μm [41–42]. MODIS data has widely been used and validated ina number of studies of Africa [18,43–45]. MCD12Q1 is available yearly at a 1 km x 1 km resolution. The yearly availability of MCD12Q1 makes it preferable in this study over Globcover, which has shown better performance in Africa, but only provides data from December, 2004 - June, 2006 and January - December 2009 [46].

The MCD12Q1 data is divided into eighteen distinct land classifications, which were converted into another set of classifications required by WetSpass-M. Of the eighteen MODIS classifications, only ten were found in the study area. A model was built in ArcGIS to convert the numbers signifying those ten MODIS classes into eight Wetspass-M classes (Table 1).

MODIS		**WetSpass-M**	
Label	**Number**	**Label**	**Number**
Rainfed Cropland	12, 14	Agriculture	21
Mosaic Vegetation	12, 14	Reference Grassland	307
Forest	6, 7	Mixed Forest	33
Shrubland	6, 7	Shrub	36
Grassland	9, 10	Reference Grassland	307
Sparse Vegetation	9, 10	Reference Grassland	307

Table 1. Conversion table of MODIS land cover class values to WetSpass-M class values.

Two different land cover datasets were created, one considering burning and one without burning. The dataset considering burning combined the land classification raster with fire counts derived from MOD14/MYD14 Collection 5 fire data. MOD14 data is derived from a fire detection algorithm which takes the two 4-μm channels, numbered 21 and 22. Classification of a pixel as containing fire ia only considered if the fire is strong enough [47–48]. For each grid cell, Terra/Day, Terra/Night, Aqua/Day, or Aqua/Night settings were selected based on which had the most fire detected; this value was then used for the day. Each daily total was then summed in order to get a monthly value per grid cell (Figures 4a and 4b).Though the monthly value represents one overpass per day, the data is quantitatively representative of the diurnal burn pattern, but does provide statistically qualitative information. The fire data were then overlaid onto the land cover map using GIS to simulate which vegetated areas were likely affected by burning.

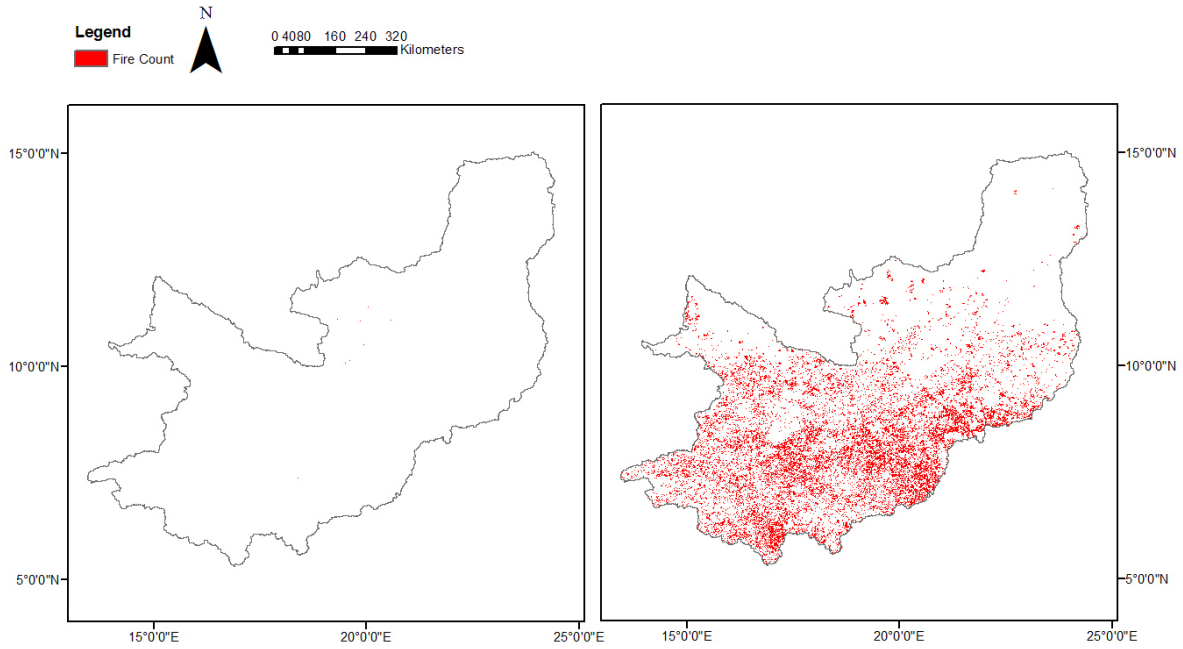

(**a**) (**b**)

Figure 4. MOD14 fire counts from dry season August 2010 (a) and burning season month January2010 (b).

A GIS model was built, which first extracted the fire count for the desired month and then created a raster of only pixels detecting fire was created using the Raster Calculator tool. Specific land cover types were extracted from the previously created yearly land cover data used in the non-burning WetSpass-M model. The extracted land cover classes were: cropland, savanna, mixed forest, deciduous forest, coniferous forest, and grassland (Figure 5a). Each land cover area was then used as a mask to extract only those areas which experienced burning. For example, a new raster for savanna was created only showing those areas in the savanna in which fire was detected for a particular month. Each of the newly created land cover rasters was then assigned a number corresponding to a WetSpass code used in the look-up table [Table A1]. The burned areas were merged with the other land cover types such as urban, bare soil, etc. and new classes were assigned to vegetated areas shown as burned: burned coniferous, burned deciduous, burned mixed forest, burned savannah, and burned grassland (Figure 5b). The land cover values were then used by WetSpass-M to assign land use parameters by means of a lookup table used in water balance calculation.

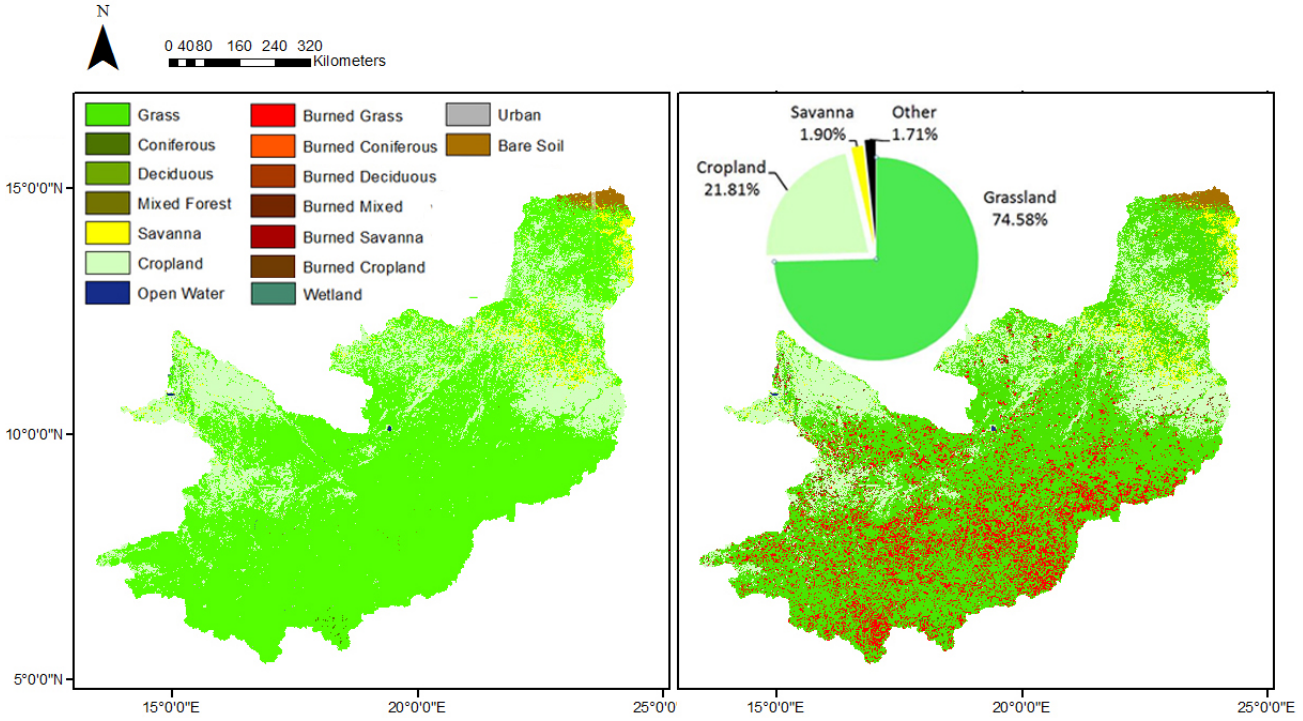

(**a**) (**b**)

Figure 5(a). Map showing January 2010 WetSpass-M land use classifications derived from MODIS MDC12Q1. **(b)** Map showing August 2010 WetSpass-M land use classifications derived from MODIS and MOD14. Pie chart shows land cover percentages in the Chari-Logone catchment derived from MDC12Q1. Grassland is by far the greatest land cover type followed by cropland. All other land cover types such as forest, bare soil, wetland, urban, and open water are combined into the category "other".

For this study, additional land cover types were included in the land use look-up table to account for burning. For example, LAI (the quantity of leaf coverage compared to ground surface area) changes to the look-up table parameters were calculated using the same method employed by [37] with the modification of the equation:

$$VC = VC_U[1 - FBA \times (1 - SR)] \quad (1)$$

where VC is the burned vegetation cover, VCu is the original (unburned) vegetation cover, FBA is the fractional burned area, and SR is the survival rate. Effected land cover parameters include LAI, vegetated area, burned area, impervious area, open water area, root depth, minimum stomata opening, vegetative height, Manning coefficient, land factor, and aerodynamic resistance. LAI is a quantity measuring the leaf area per unit of ground surface area. LAI modifies the amount of water from precipitation and heat fluxes, affecting ET and runoff. Minimum stomata opening refers to the minimum size of stomata for that land cover type. Stomata, which are the pores on leaves used for gas exchange, have been shown to change size with temperature depending on water availability [49]. Burning also reduces vegetative height as land is cleared of vegetation, and thus increasing wind speed. Increased wind speed reduces sensible heat, increasing leaf temperature and stomatal resistance, thus increasing transpiration. Conversely, decreased vegetative height tends to decrease aerodynamic resistance, also known as drag. Aerodynamic resistance is calculated for the WetSpass-M table using:

$$r_a = \frac{1}{K^2 U_a Z_a}\left(ln\left(\frac{Z_a - Z_d}{Z_0}\right)\right)^2 \quad (2)$$

where r_a is the aerodynamic resistance, K is the von Karman constant (0.41), U_a is the wind speed at elevation Z_a, Z_d is the zero displacement elevation , and Z_0 is the aerodynamic roughness height of surface [34]. Decreased aerodynamic resistance has the effect of decreasing ET [50].

Analysis of land use model inputs for the CLC show the dominant classes to be grassland (74.88%), cropland (21.81%), and savanna (1.90%). Coniferous, deciduous, and mixed forest combined only make up 0.12%, with wetland covering 0.2%. Non-vegetative cover are open water (0.28%), urban build-up (0.18%), and bare soil (0.93%) (Figure 5 (b)).

Burning within the dominant land cover types show grassland to have the highest fire detection with an average of 5%-20% of grassland showing fire during the dry season. Grassland fires may be due to controlled burning or wildfires, but that they make up such a large portion of the catchment is significant. Peak burning appears to occur from November through January for all classes with little to no burning occurring May through July (Figure 6).

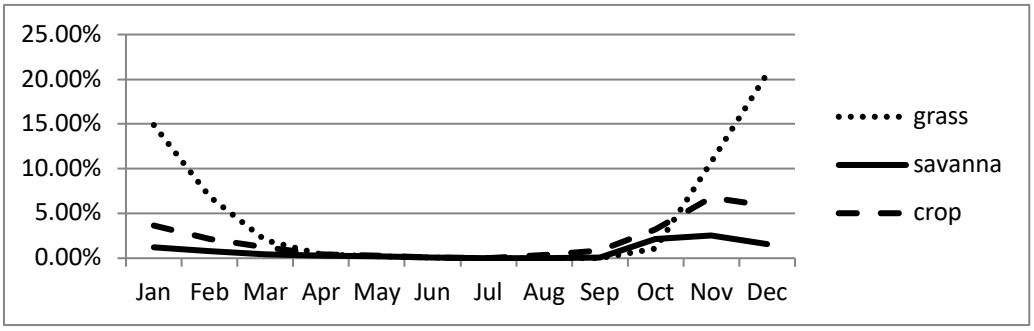

Figure 6. Average percent of monthly burning for major land cover types from 2003-2011 taken from MOD14.

Temperature data was extracted from the MOD11C3 Version 5 monthly daytime CMG land-surface temperature product from MODIS Terra. MOD11C3 is derived from the MOD11C1 daily global product, taking daily clear sky land surface temperature values and averaging them for a month at 0.05 degree resolution (~5.56 km). Validation of MODIS land surface temperature has been well researched [51–53]. Hulley and Hook [54] show the high degree of MODllC1 accuracy in Africa by comparing the data to in situ measurements taken in Namibia, Botswana, and South Africa. MODllC1 Version 5 showed a mere 1.93% combined mean temperature difference to ground measurements. Analysis of land surface temperature shows a decrease in temperature during the wet season due to the cooling effect of precipitation over land.

Global climate models, such as the Global Forecast System (GFS) or Modern-Era Retrospective analysis for Research and Applications (MERRA), have the capability to calculate wind speed at various atmospheric layers. Unfortunately, GFS has a relatively low resolution of 28 km, which is far too coarse for this study. Custom climate models such as a Weather Research and Forecasting (WRF) model could be built for the study area. However, this was beyond the scope of the study and, even then, such models have difficulty accounting for the complex terrain when calculating near surface winds at a desired resolution [55–56]. For these reasons, station data were used for wind speed despite issues with data continuity. NOAA does not provide monthly wind speed averages, so daily records from NCEI Global Summaries of the Day were used and averaged monthly. The average wind speed values were also converted from 0.1 knots to m/s.

Once the wind speed data was averaged, it was imported into ArcGIS as a shapefile and converted to a raster using kriging [57]. The data was then processed and converted into the proper format for input into WetSpass-M.

PET is the maximum evaporation and transpiration that could occur assuming sufficient water. As noted earlier, burning has a significant impact on surface albedo change. This change in albedo affects the energy balance and therefore should not be overlooked when calculating PET. Two PET datasets were created for use for the two WetSpass-M models. Albedo values considering burned and non-burned vegetative classes were derived from [16] and those of non-vegetative areas are taken from Yu and Lu [58]. The spatial distribution of albedo was assigned using the modified MDC12Q1 (Type1) yearly land cover data showing burned areas. To consider the effect of albedo change on PET, a simplified penman equation was used following the method outlined by Valiantzas[59]:

$$E_{PEN} \approx 0.051(1-\alpha)R_S\sqrt{T+9.5} - 2.4\left(\frac{R_S}{R_A}\right)^2 + 0.052(T+20)\left(1-\frac{RH}{100}\right)(a_u - 0.38 + 0.54u) \quad (3)$$

where E_{PEN} is the Penman potential evapotranspiration, α is the albedo, R_s is the solar radiation, T is the surface temperature, R_A is the extraterrestrial radiation, RH is the relative humidity, a_u is a wind function coefficient of 1, and u is the wind speed. The wind coefficient of 1, was used originally used by Penman [60]. Since no solar radiation is available from regional station data, it is estimated from measured sunshine hours using the equation:

$$R_S = R_A \times \left(0.5 + 0.25 \times \frac{n}{N}\right) \quad (4)$$

where n is the measured bright sunshine hours per day, and N is the maximum possible duration of daylight which is derived from the latitude of the site and the number of Julian months are given [61–62]. R_A is calculated using:

$$R_A = 37.59 d_r[\omega_S \sin(\phi)\sin(\delta) + \sin(\omega_S)cos(\phi)cos(\delta)] \quad (7)$$

where d_r is the relative distance between the sun and the earth, ϕ is the radians, and δ is the solar declination. Maximum possible duration of daylight is calculated using the equation:

$$N = \frac{24}{\pi}\omega_S \quad (8)$$

where ω_S is the sunset hour angle in radians. δ is the solar declination and is determined using:

$$\delta = 0.409\sin\left(\left(\frac{2\pi}{365}\right)J - 1.39\right) \quad (9)$$

where$J$ is the Julian day corresponding to the respective month [60–61]. Relative humidity was calculated using the equation:

$$RH = 100\left(\frac{e_a}{e^{\circ}(T)}\right) \quad (10)$$

where $e^{\circ}(T)$ is the saturation vapor pressure (kPa) and e_a is the actual vapor pressure.

Climate station data from NCEI Global Summaries of the Month were used to calculate solar radiation, extraterrestrial radiation, and relative humidity and these values were used to create raster datasets. The data were imported into GIS and a model was used to calculate the two PET datasets and export them for use as WetSpass-M inputs. PET was validated by comparing the calculated PET to Consultative Group for International Agricultural Research (CGIAR-CSI) PET, which averages PET observations from 1950 - 2000 [63–64]. Calculated PET with albedo matched well against the CGIAR PET [Figure S1].

Elevation from a digital elevation model (DEM) was provided by the Shuttle Radar Topography Mission (SRTM). The Shuttle Radar Topography Mission (SRTM) is an international project coordinated by the National Imagery and Mapping Agency (NIMA) and NASA [65]. The primary objective of the mission was the acquisition a complete high-resolution digital topographic database of the Earth. SRTM flew onboard the Space Shuttle Endeavour consisted of a specially modified radar system and had an 11-day mission in February of 2000. The digital topographic map products were designed to meet Interferometric Terrain Height Data (ITHD) specifications: with 30 m x 30 m spatial sampling and absolute vertical height accuracy (90% linear error) of 16 m. The absolute horizontal accuracy (90% circular error) is 20 m. The SRTM resolution used in this study is 90 m x 90 m (Sun et al., 2003). Slope was calculated using the elevation input by the WetSpass-M program.

Lastly, a groundwater raster dataset was generated using 2009 measurements taken from a collaborative study in the Lake Chad Basin by the University of Missouri, Kansas City and NASA Goddard Space Flight Center and [66]. The data were imported into ArcGIS and converted to shapefile points and converted to raster using kriging. This same data was used by Babamaji [6].

3. Results

3.1 Validation

We performed model validation by comparing runoff outputs from Wetspass-M to the Logone river discharge measurements acquired at the Bongor station during2003 to 2007 [67]. A Nash-Sutcliffe Efficiency (NSE) of 0.57 was found for the data sets, indicating that the model did well in calculating hydrological parameters (Figure S2 (a)), where a value between 0 and 1 is considered good with 1 being the perfect match [68]. An r^2 value of 0.68 (Figure S2(b)) found between the measured and calculated value was satisfactory.

3.2 Analysis

Analysis of the model results considering albedo change from burning shows the majority of precipitation being distributed to ET and recharge. The majority of available water from precipitation are lost to ET (45.19%) and groundwater recharge (45.35%), leaving a smaller portion available for surface runoff. We determined the burning impact by subtracting the monthly average outputs of without burning from with burning for 2003 to 2011.

To get a more detailed understanding of fire effect in the CLC, an investigation of the effect of fire by land cover type was performed. Particular attention was paid to the three primary land cover classes in the study area: grassland, savanna, and cropland. Average wet season ET decreased 7.56E+18 mm per month and a decrease 3.47 mm/day or 1.06E+19 mm per month for the dry season. This is in agreement with other research [69–70], who found that ET was especially reduced by burning during the early monsoonal season. Increases in ET, recharge, and runoff due to fire were observed in the dry season and can be attributed primarily to grassland burning (Figures 7a & 7b). Consid-

ering burning, grassland, shows an increase in ET and recharge during the dry season but they show a decreasing pattern in the wet season. These parameters have an increase in runoff during the wet season (Figure 7b).

Considering no burning, there is more ET observed during the wet season in savanna, whereas there is less ET, more runoff, and more recharge when considering burning (Figure 7c). Cropland shows more runoff, but less recharge and ET during the wet season (Figure 7d).

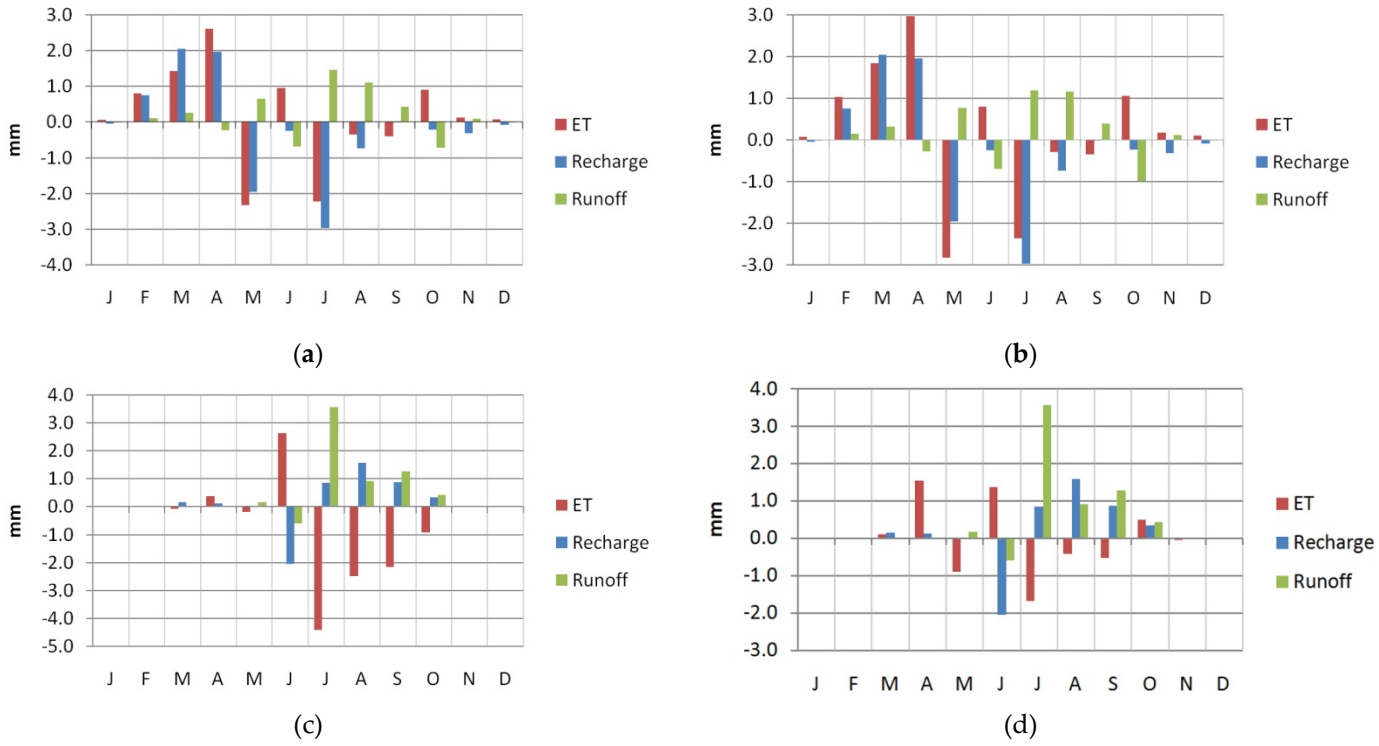

Figure 7. Average monthly output difference of hydrological parameters from non-burning model subtracted from the model considering burning. Top to bottom panels show burning difference for: (a) all land classes, (b) grassland, (c) savannah, (d) cropland.

To take the amount of monthly fire distribution into account MODIS MOD14/MYD14 fire count data were compared to water cycle indicators using general linear least squares regression analysis [Figure 8]. Correlation between annual burning changes to water balance parameters are negative. This matches findings by Ichoku [18] and supports the idea that with increased severity of fire, there is a severe decrease in hydrologic parameters including precipitation.

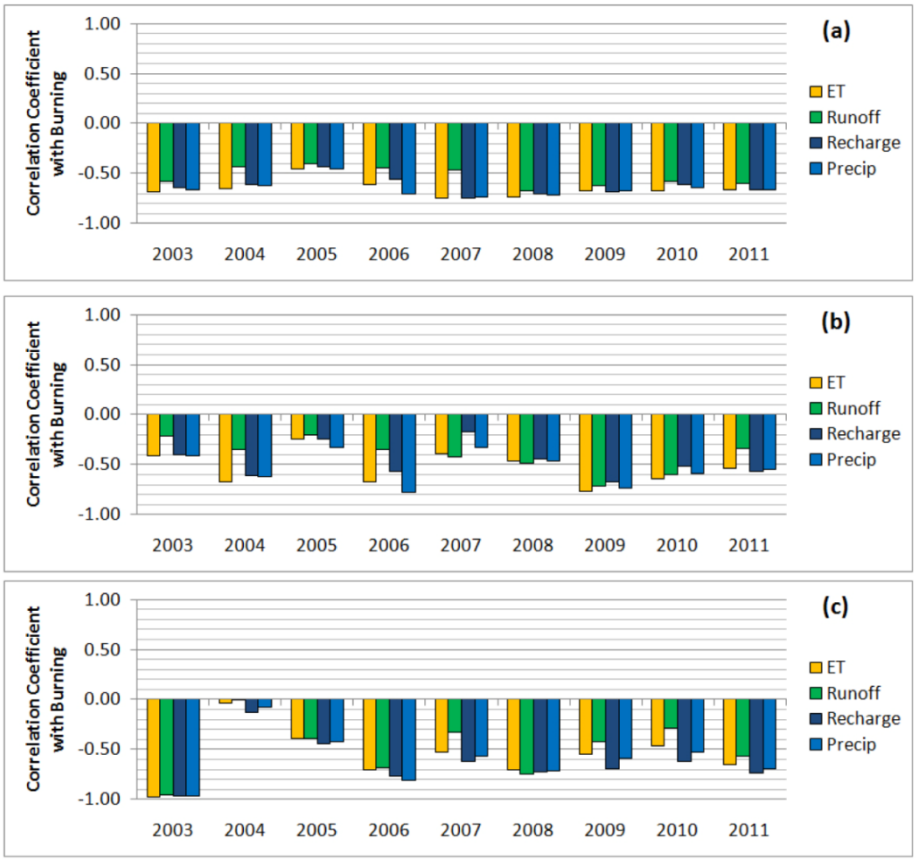

Figure 8. Correlation coefficients between biomass burning count (each count being 2km x 2km pixel) from MOD14/MYD14 Collection 5 compared to water balance model outputs considering burning based on different time periods: (a) integration or averaging through the full-year cycle and, (b) integration or averaging through only the dry season (November–March), (c) integration or averaging through only the wet season (April–October).

To minimize the effects of quantitative biases and uncertainties, correlations between fire count and water-cycle parameters were calculated for the dry season and wet season. Both seasons showed a consistent negative correlation between fire count and water-cycle parameters. The dry season findings differ from what was found in the Ichoku [18] study. However, it should be noted that the study area of the entire North Central block included significant wetland converted to agriculture, especially near the LCB. The CLC has very little wetland making up a mere 0.2% of total land coverage; the majority wetlands of the LCB lie to the northwest of this area. Therefore, it is reasonable to presume that changes due to wetland conversion to cropland mentioned by Ichoku [18] would not be observed since the land cover is different in this regard. Results from a scatter plot of fire count against precipitation for the CLC shows that burning has an inverse relationship with precipitation [Figure 9]. The results look remarkably similar to those found by Ichoku [18] and further emphasize the inverse relationship between burning and monsoonal rainfall.

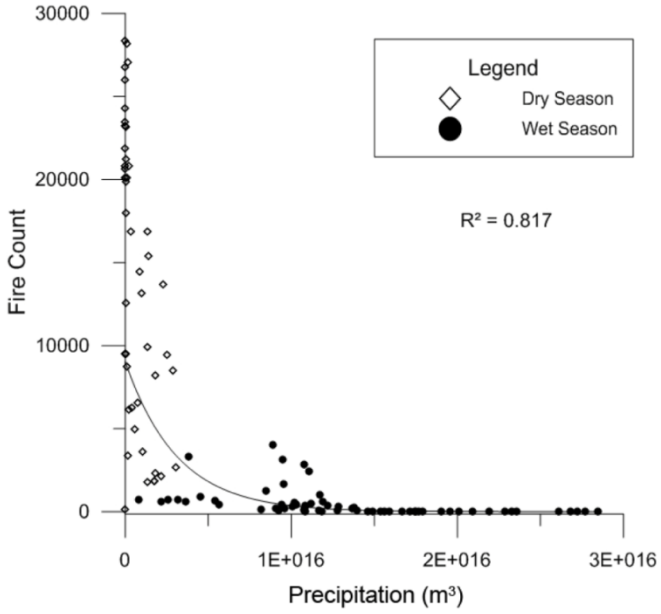

Figure 9. Scatter plot of monthly biomass burning count against precipitation from TRMM showing the demarcation between the monsoonal season (May–October) and dry season (November–March) season.

The ability of WetSpass-M to approximate discharge found in situ shows great promise of using it to calculate hydrological parameters despite severe lack of data. By the use of satellite data in lieu of meteorological station records, temporal and spatial data limitations may be mitigated. Development of a system to incorporate albedo into PET calculations at a relatively high resolution may prove useful for future studies examining the impact of burning on albedo and land cover type.

4. Discussion

When comparing model simulations with and without fire activity considerations, a clear pattern of decreased ET is observed in the burning model. However, lower ET may limit the water available for precipitation and could have significant meteorological impacts on agriculture, though more study in this area is needed.Burning seems to also have an impact on the primary land cover types of the CLC, which in turn, gave a significant impact on hydrological parameters. Analysis of the burning scenario show that burning grassland, which composes almost 75% of Chari-Logone total land cover, causes increased ET and runoff during winter months. Recent studies have demonstrated the increasing trend in LCB of converting shrubland, grassland, and wetlands to cropland. This change from grassland to cropland has the potential of decreasing water available to water bodies during the winter.

The ability of WetSpass-M to approximate discharge found *insitu* shows great promise for using it to calculate hydrological parameters despite severe lack of data. By the use of satellite data, in lieu of meteorological station records, temporal and spatial limitations may be mitigated. Development of a system to incorporate albedo into PET calculations at a relatively high resolution may prove useful for future studies examining the impact of burning on albedo and land cover type, as well as on the hydrological cycle.

5. Conclusion

Burning and no-burning models were used in WetSpass-M to determine the affect of burning on land classes. The affect of burning varied by vegetative type and whether the burning occurred during the dry or wet season in LCB. A negative correlation of fire to

water cycle was clearly observed. Water balance is affected by land cover, with each land cover responding differently to burning. If the pattern of converting shrubland to cropland continues, the primary difference will be less groundwater recharge. Since grassland constitutes the majority of landcover in the CLC, it is worth noting that burning increases ET and recharge during the dry season but decreases ET and recharge wet season. These parameters have an increase in runoff during the wet season. This research provides insight into how burning affects different land use types within a critical region of the LCB since it provides a significant amount of water to Lake Chad. All vegetative classes in a burning scenario showed a decrease in ET during the wet season, supporting the idea that, with increased burning, there would be a severe decrease of precipitation.

Further research detailing the groundwater recharge along the Chari and Logone rivers would be beneficial to understanding the hydrology of the CLC in relation to fire, but would probably need more detailed field data for rainfall and wind, as well as groundwater measurements. A greater distribution of these measurements increasing in number near the confluence of the Chari and Logone Rivers and near their combined discharge to Lake Chad would be beneficial. If more data for burning to non-burning albedo comparisons would become available, a longer study period could allow for better analysis of the effect of land cover change on burning in the CLC.

Supplementary Materials: The following are available online at www.mdpi.com/xxx/s1, Figure S1: title, Table S1: title, Video S1: title.

Author Contributions: Forrest Black developed the methodology and conducted the work under the supervision and review of Jejung Lee. Jejung Lee also conceptualized this project. Charles Ichoku provided project coordination and acquired funding. Luke Ellison provided MOD14 fire count data and Charles Gatebe provided surface albedo data. Rakiya Babamaaji provided initial guidance for preparing GIS data. Khodayar Abdollahi provided technical WetSpass-M software and technical guidance. Soma San contributed to data processing. All authors contributed feedback and development of this manuscript.

Funding: This research was fully funded by NASA Interdisciplinary Studies (IDS) Program (Dr Jack Kaye, Earth Science Research Director) through the Radiation Sciences Program managed by Dr Hal Maring.

Data Availability Statement: The data that support the findings of this study are available from the corresponding author upon reasonable request..

Conflicts of Interest: The authors declare no conflict of interest.

Supplementary

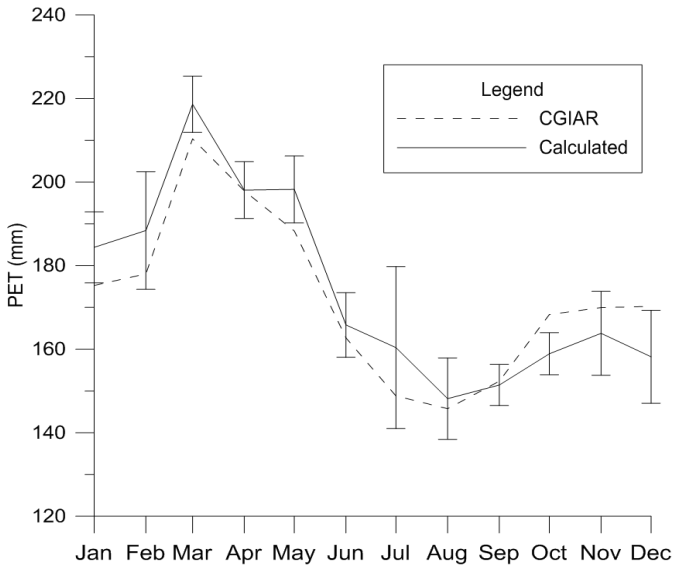

Figure S1. Comparison of averaged PET by month using the modified Penman equation for 2003-2011 compared to CGIAR-CSI worldwide monthly averages from 1950-2000.

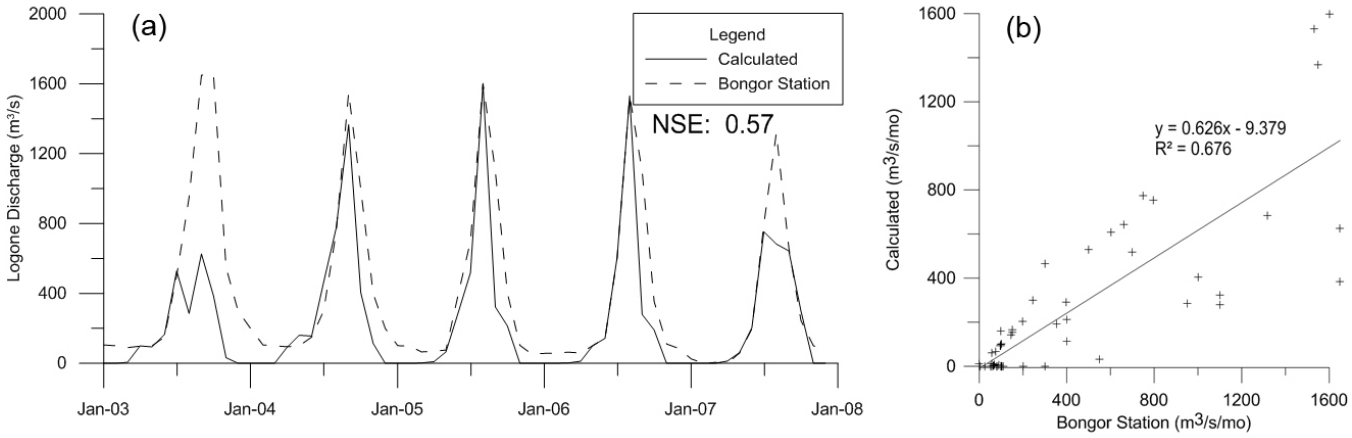

(**a**) (**b**)

Figure S2. In situ monthly Logone river discharge data from Bongor station compared to WetSpass-M outputs considering burning (a). Scatter plot of monthly discharge data from 2003 to 2011 for Bongor station compared to model outputs considering burning (b).

Table A1. WetSpass-M Vegetative Land Lookup Table.

Land Use Type	Vegetated Runoff	Vegetated Area	Bare Area	Impervious Area	Open Water Area	Root Depth	LAI	Min Stomata Opening	Vegetative Height	nManing	Land Factor	Aerodynamic Resistance
cropland	crop	0.8	0.2	0	0	0.4	4	180	0.6	0.037	0.541	115.013
burned cropland	crop	0	1	0	0	0.4	0	180	0.6	0.02	0.541	115.013
deciduous forest	forest	1	0	0	0	2	5	250	18	0.1	0.2	27.196
burned deciduous	forest	0.75	0.25	0	0	2	5	250	18	0.02	0.2	27.196
coniferous forest	forest	1	0	0	0	2	6	500	15	0.1	0.2	28.631
burned coniferous	forest	0.75	0.25	0	0	2	5	500	15	0.02	0.2	28.631
mixed forest	forest	1	0	0	0	2	5	375	16	0.1	0.2	28.098
burned mixed forest	forest	0.75	0.25	0	0	2	4	375	16	0.02	0.2	28.098
savannah	grass	1	0	0	0	0.6	6	110	2	0.05	0.4	66.329

burned savanna	grass	0.15	0.85	0	0	0.6	5	110	2	0.02	0.4	66.329
grass	grass	1	0	0	0	0.3	2	140	0.12	0.035	0.571	212.014
burned grass	grass	0	1	0	0	0.3	0	140	0.12	0.02	0.571	212.014

References

1. Okonkwo, C., Demoz, B., Sakai, R., Ichoku, C., Anarado, C. and Adegoke, J. (2015). Combined effect of El Niño southern oscillation and Atlantic multidecadal oscillation on Lake Chad level variability. Cogent Geoscience ,Volume 1, 2015 - Issue 1.
2. Musa I. K. (2008). Saving Lake Chad. Proceedings of Sirte Roundtable. Lake Chad Basin
3. Sarch M. T. (2001) Fishing and farming at Lake Chad: Institutions for access to natural resources. Journal of Environmental Management, 62(2), pp. 185–199, https://doi.org/10.1006/jema.2001.0430.
4. Kimmage K. & Adams W. M. (1992). Wetland Agricultural Production and River Basin Development in the Hadejia-Jama'are Valley, Nigeria. The Geographical Journal 158: pp. 1–12.
5. Food and Agricultural Organization. (2009). Adaptive water management in the Lake Chad Basin: Addressing current challenges and adapting to future needs. Food and Agriculture Organization (FAO) Water Seminar Proceedings. World Water Week, Stockholm, August 16-22, 10-19.
6. Babamaaji R. A., & Lee J. (2014). Land use/land cover classification of the vicinity of Lake Chad using NigeriaSat-1 and Landsat data. Environmental Earth Sciences, 71(10), 4309-4317. doi:10.1007/s12665-013-2825-xnd Envir. 126: pp. 67–80.
7. Bouchez C., Goncalves J., Deschamps P., Vallet-Coulomb C., Hamelin B., DoumnangJ.,...&Sylvestre, F. (2016). Hydrological, chemical, and isotopic budgets of Lake chad: A quantitative assessment of evaporation, transpiration and infiltration fluxes. Hydrology and Earth System Sciences, 20(4), pp. 1599–1619. doi:10.5194/hess-20-1599-2016.
8. Nicholson, S. (2013). The West African Sahel: a review of recent studies on the rainfall regime and its interannual variability. ISRN Meteorology. (453521).
9. Nicholson, S. E., Some, B., & Kone, B. (2000). An analysis of recent rainfall conditions in west Africa, including the rainy seasons of the 1997 el nino and the 1998 la nina years. Journal of Climate, 13(14), 2628–2640.
10. Policelli F, Hubbard A, Jung HC, Zaitchik B, Ichoku C (2018). Lake Chadtotal surface water area as derived from land surface temperature andradar remote sensing data. Remote Sens 10(2):252.
11. Thonicke K., Venevsky S., Sitch S., &Cramer W. (2001). The role offire disturbance for global vegetation dynamics: coupling fireinto a dynamic global vegetation model. Global Ecology and Biogeography10: pp. 661–677.
12. Lyons E., Jin Y., &Randerson J. (2008) Changes in surface albedo afterfire in boreal forest ecosystems of interior Alaska assessed usingMODIS satellite observations. Journal of Geophysical Research 113:G02012.doi:10.1029/2007JG000606.
13. Bowman D., Balch J., Artaxo P., Bond W., Carlson J., Cochrane M., ...&Pyne S. (2009). Fire in the earth system. Science 324: pp. 481–484.
14. Ichoku C., & Ellison, L. (2014). Global top-down smoke-aerosol emissions estimation using satellite fire radiative power measurements. Atmospheric Chemistry and Physics, 14(13), pp. 6643–6667. doi:10.5194/acp-14-6643-2014.
15. van der Werf G. R., Randerson J. T., Giglio L., Collatz G.J., Mu M.,Kasibhatla P. S., . . .&van Leeuwen T. T.(2010) Global fire emissions and thecontribution of deforestation, savanna, forest, agricultural,and peat fires (1997–2009) Atmospheric Chemistry and Physics. 10,pp. 11707–11735.
16. Gatebe C. K., Ichoku C. M., Poudyal R., Román M. O., & Wilcox E. (2014). Surface albedo darkening from wildfires in Northern Sub-Saharan Africa. Environmental Research Letters, 9 065003.
17. De Sales F., Xue Y., &Okin G. S. (2016). Impact of burned areas on the northern African seasonal climate from the perspective of regional modeling. Climate Dynamics, 47(11), pp. 3393–3413. doi:10.1007/s00382-015-2522-4.
18. Ichoku C., Ellison L. T., Willmot K. E., Matsui T., Dezfuli A. K., Gatebe C. K., . . . & Habib S. (2016). Biomass burning, land-cover change, and the hydrological cycle in northern sub-saharan Africa. Environmental Research Letters, 11(9), doi:10.1088/1748-9326/11/9/095005.
19. Gao H., Bohn T. J., Podest E., McDonald K. C., &Lettenmaier D. P. (2011). On the causes of the shrinking of Lake Chad. Environmental Research Letters, 6(3). doi:10.1088/1748-9326/6/3/034021.
20. Vuillaume G. (1981). Bilanhydrologiquemensuel et modélisationsommaire du régime hydrologique du lac Tchad. Paris. Cah. ORSTOM, Série Hydrologie, 18(1), pp.23–72. ISSN 0008-0381.
21. Govaerts Y., Pereira J., Pinty B., &Mota B. (2002). Impact of fires on surface albedo dynamics over the African continent. Journal of Geophysical Research-Atmospheres 107(D22), 4629. doi:10.1029/2002JD002388.
22. Myhre G, Govaerts Y, Haywood J, Berntsen T, &Lattanzio A (2005) Radiative effect of surface albedo change from biomass burning. Geophysical Research Letters 32:L20812. doi:10.1029/2005GL022897.
23. Saha M. V., D'Odorico P., & Scanlon T. M. (2017). Albedo changes after fire as an explanation of fire-induced rainfall suppression. Geophysical Research Letters, 44(8), pp. 3916–3923. doi:10.1002/2017GL073623.

24. De Bano L. F. (1981). Water repellent soils: A state-of-the-art. US Department of Agriculture. Forest Service, General Technical Report, (PSW-46).
25. Rulli M. C., Offeddu L., & Santini, M. (2013). Modeling post-fire water erosion mitigation strategies. Hydrology and Earth System Sciences, 17(6), pp. 2323–2337. doi:10.5194/hess-17-2323-2013.
26. Nyman P., Smith H. G., SherwinC. B., Langhans C., Lane P. N. J., & Sheridan, G. J. (2015). Predicting sediment delivery from debris flows after wildfire. Geomorphology, 250, pp. 173–186. doi:10.1016/j.geomorph.2015.08.023.
27. Buma W. G., Lee S., &Seo J. Y. (2016). Hydrological evaluation of Lake Chad basin using space borne and hydrological model observations. Water (Switzerland), 8(5) doi:10.3390/w8050205.
28. Ndehedehe, C. E., Awange, J. L., Kuhn, M., Agutu, N. O., & Fukuda, Y. (2017). Climate teleconnections influence on West Africa's terrestrial water storage. Hydrological Processes, 31(18), pp. 3206-3224. doi:10.1002/hyp.11237.
29. Ramillien G., Frappart F., &Seoane L. (2014). Application of the regional water mass variations from GRACE satellite gravimetry to large-scale water management in Africa. Remote Sensing, 6(8), pp. 737977–867405. doi:10.3390/rs6087379.
30. SkaskevychA.,LeeJ.,JungH.C.,BoltenJ.,DavidJ. L. ,PolicelliF. S. ,GoniI. B. ,FavreauG,SanS.,IchokuC. M. (2020)ApplicationofGRACEto the estimation of groundwater storage change in a data-poorregion: a case study of Ngadda catchment in the Lake ChadBasin. Hydrol Process 34:941–955.
31. Eklund L., Romankiewicz C., Brandt M., Doevenspeck M., &Samimi C. (2016). Data and methods in the environment-migration nexus: A scale perspective. Erde, 147(2), pp. 139–152. doi:10.12854/erde-147-10.
32. Sanogo S., Fink A. H., Omotosho J. A., Ba A., Redl, R., &Ermert V. (2015). Spatio-temporal characteristics of the recent rainfall recovery in West Africa. International Journal of Climatology, 35(15), pp. 4589–4605. doi:10.1002/joc.4309.
33. Zhang W., Brandt M., Guichard F., Tian Q., &Fensholt R. (2017). Using long-term daily satellite based rainfall data (1983–2015) to analyze spatio-temporal changes in the sahelian rainfall regime. Journal of Hydrology, 550, pp. 427–440. doi:10.1016/j.jhydrol.2017.05.033.
34. Batelaan O., & De Smedt F. (2007). GIS-based recharge estimation by coupling surface-subsurface water balances. Journal of Hydrology, 337(3-4), pp. 337–355. doi:10.1016/j.jhydrol.2007.02.001.
35. Abdollahi K., Bashir I., Verbeiren B., Verbeiren B., Harouna M. R., Van Griensven A., Huysmans M., Batelaan O. (2017). A distributed monthly water balance model: formulation and application on Black Volta Basin . Environmental Earth Sciences, 76: 198. https://doi.org/10.1007/s12665-017-6512-1.
36. Melki A., Abdollahi K., Fatah R., & Habib A. (2017). Groundwater recharge estimation under semi arid climate: Case of Northern Gafsa watershed, Tunisia.Journal of African Earth Sciences, 132, pp. 37–46. https://doi.org/10.1016/j.jafrearsci.2017.04.020.
37. De Sales F., Xue Y., &Okin G. S. (2016). Impact of burned areas on the northern African seasonal climate from the perspective of regional modeling. Climate Dynamics, 47(11), pp. 3393–3413. doi:10.1007/s00382-015-2522-4.
38. Li, M., & Shao, Q. (2010), An improved statistical approach to merge satellite rainfall estimates and raingauge data. Journal of Hydrology, 385, 51–64, https://doi.org/10.1016/j.jhydrol.2010.01.023.
39. Pombo, S.,&Proença de Oliveira, R. (2015). Evaluation of extreme precipitation estimates from TRMM in Angola. Journal of Hydrology, 523, 663–679, https://doi.org/10.1016/j.jhydrol.2015.02.014.
40. Ojo, J. S., &Omotosho, T. V. (2013). Comparison of 1-min rain rate derived from TRMM satellite data and rain gauge data for microwave applications in Nigeria. Journal of Atmospheric and Solar-Terrestrial Physics, 102, 17–25, https://doi.org/10.1016/j.jastp.2013.04.008.
41. Friedl M.A., McIver D.K., Hodges J.C., Zhang X., Muchoney D., Strahler A.H., ... & Cooper, A. (2002). Global land covermapping from MODIS: algorithms and early results. Remote Sensing of Environment 83, pp. 287–302.
42. Friedl M.A., Sulla-Menashe D., Tan B., Schneider A., Ramankutty N., Sibley A., & Huang, X. (2010). MODIS collection 5 global land cover: algorithm refinements and characterization of new datasets. Remote Sensing of Environment 114, pp. 168–182.
43. Al-Hamdan M.Z., Oduor, P., Flores A.I., Kotikot S.M., Mugo R., Ababu J., & Farah H. (2017). Evaluating land cover changes in Eastern and Southern Africa from 2000 to 2010 using validated Landsat and MODIS data. International Journal of Applied Earth Observation and Geoinformation 62, pp. 8–26, https://doi.org/10.1016/j.jag.2017.04.007.
44. Gessner U., Bliefernicht J., Rahmann M., &DechS .(2012). Land cover maps for regional climate modeling in West Africa—a comparison of datasets. Proceedings of the 32nd Annual EARSeL Symposium. Mykonos, Greece, May 21–25.
45. Vintrou E., Desbrossea A., Beguea A., Traoreb S., Barona C., &Seena D., (2012). Crop area mapping in West Africa using landscape stratification of MODIS time series and comparison with existing global land products. International Journal of Applied Earth Observations and Geoinformation 14, pp. 83–93.
46. Yang Y., Xiao P., Feng X., & Li H. (2017). Accuracy assessment of seven global land cover datasets over China. ISPRS Journal of Photogrammetry and Remote Sensing 125, pp. 156–173, https://doi.org/10.1016/j.isprsjprs.2017.01.016.
47. Giglio L., Descloitres J., Justice C. O., & Kaufman Y. J. (2003). An enhanced contextual fire detection algorithm for MODIS. Remote Sensing of Environment, 87(2-3), pp. 273–282. doi:10.1016/S0034-4257(03)00184-6.
48. Justice, C. O., Giglio, L., Korontzi, S., Owens, J., Morisette, J. T., Roy, D., Descloitres, J., Alleaume, S., Petitcolin, F., & Kaufman, Y. (2002). The MODIS fire products. Remote Sensing of Environment, 83, 244–262.
49. Schulze, E. D., &Küppers, M. (1979). Short-term and long-term effects of plant water deficits on stomatal response to humidity in Corylusavellana L. Planta 146, 319–326,doi: 10.1007/BF00387804.

50. Li, F., Lawrence, D.M., & Bond-Lamberty, B. (2018).Human impacts on 20th century fire dynamics and implications for global carbon and water trajectories. Global and Planetary Change, 162, 18-27. https://doi.org/10.1016/j.gloplacha.2018.01.002.
51. Bosilovich, M. G. (2006).A comparison of MODIS land surface temperature with in situ observations, Geophysical Research Letters, 33, L20112, doi:10.1029/2006GL027519.
52. Coll, C., Wan, Z., & J. M. Galve. (2009).Temperature-based and radiance-based validations of the V5 MODIS land surface temperature product. Journal of Geophysical Research, 114, D20102, doi:10.1029/2009JD012038.
53. Wan, Z., & Li, Z. L. (2010). Radiance-based validation of the V5 MODIS land-surface temperature product. International Journal of Remote Sensing, 29(17–18), 5373–5395, DOI: 10.1080/01431160802036565.
54. Hulley, G. C. & Hook, S.J. (2009). Intercomparison of versions 4, 4.1 and 5 of the MODIS Land Surface Temperature and Emissivity products and validation with laboratory measurements of sand samples from the Namib desert, Namibia. Remote Sensing of Environment, 113, 1313-1318, https://doi.org/10.1016/j.rse.2009.02.018.
55. Engelstaedter, S., & Washington, R. (2014). Evaluation of reanalysis near-surface winds over northern Africa in Boreal summer. EGU General Assembly 2014 April 27 - Vienna, Austria, id.13169.
56. Mughal, M. O., Lynch, M., Yu, F., McGann, B., Jeanneret, F., &Sutton, J. (2017). Wind modelling, validation and sensitivity study using weather research and forecasting model in complex terrain. Environmental Modelling & Software, 90, 107–125. https://doi.org/10.1016/j.envsoft.2017.01.009.
57. Oliver, M. A. (1990). Kriging: A Method of Interpolation for Geographical Information Systems. International Journal of Geographic Information Systems 4, 313–332.
58. Yu X., & Lu C. (2014). Urban percent impervious surface and its relationship with land surface temperature in Yantai City, China. IOP Conference Series: Earth and Environmental Science (EES), 17(1), p. 7. doi:101088/1755-1315/17/1/012163.
59. Penman H.L. (1963). Technical communication No. 53. Commonwealth Bureau of Soils. Harpenden, Harpenden, England.
60. Valiantzas J. D. (2006). Simplified versions for the penman evaporation equation using routine weather data. Journal of Hydrology, 331(3-4), pp. 690–702, doi:10.1016/j.jhydrol.2006.06.012.
61. Shuttleworth W.J. (1993). In: Maidment, D.R. (Ed.), Evaporation. McGraw-Hill, New York, pp. 4.1–4.53 (Chapter 4).
62. Allen, R. G., Smith, M., Pereira, L.S., & Perrier, A., (1994). An update for the calculation of reference evapotranspiration. ICID Bull. 43(2), 35–92.
63. Zomer R. J., Bossio D. A., Trabucco A., Yuanjie L., Gupta D. C.& Singh V. P.(2007). Trees and Water: Smallholder Agroforestry on Irrigated Lands in Northern India. Colombo, Sri Lanka: International Water Management Institute.p 45. (IWMI Research Report 122).
64. Zomer R. J, Trabucco A., Bossio D. A., van Straaten O., &Verchot L. V.(2008). Climate Change Mitigation: A Spatial Analysis of Global Land Suitability for Clean Development Mechanism Afforestation and Reforestation. Agriculture, Ecosystems, and Environment, 126, pp. 67–80.
65. vanZyl, J. J. (2001). The Shuttle Radar Topography Mission (SRTM): A breakthrough in remote sensing of topography. Acta Astronautica, 48(5 – 12), 559–565.
66. Federal Institute of Geosciences and Natural Resources & Lake Chad Commission (2010). Lake Chad sustainable water management project activities - report N° 3. https://www.whymap.org/EN/Themen/Wasser/Projekte/abgeschlossen/TZ/Tschad/report_3.pdf?__blob=publicationFile&v=3
67. Seeber K. (2013). 2nd Mission on Discharge Measurements at Chari, Logone and Koulambou River, Chad. 2010.2274.8. BGR-No.: 05-2355.
68. Oliver F. C. & Singels A. (2012). The effect of crop residue layers on evapotranspiration, growth and yield of irrigated sugarcane. Water SA38(1), pp.77–86.
69. Moriasi, D., Gitau, M., Pai, N. and Daggupati, P. (2015). Hydrologicand water quality models: Performance measures and evaluation criteria. American Society of Agricultural and BiologicalEngineers, 58(6), 1763–1785. https://doi.org/10.13031/trans.58.10715
70. Notaro M., Wyrwoll K.-H., & G. Chen. (2011), Did aboriginal vegetation burning impact on the Australian summer monsoon? Geophysical Research Letters, 38, L11704, doi:10.1029/2011GL047774.